

## Magnetism and magnetoelectricity of a U-type hexaferrite $\text{Sr}_4\text{Co}_2\text{Fe}_{36}\text{O}_{60}$

K. Okumura, T. Ishikura, M. Soda, T. Asaka, H. Nakamura et al.

Citation: *Appl. Phys. Lett.* **98**, 212504 (2011); doi: 10.1063/1.3593371

View online: <http://dx.doi.org/10.1063/1.3593371>

View Table of Contents: <http://apl.aip.org/resource/1/APPLAB/v98/i21>

Published by the American Institute of Physics.

### Related Articles

Ferroelectric/ferromagnetic ceramic composite and its hybrid permittivity stemming from hopping charge and conductivity inhomogeneity

*J. Appl. Phys.* **113**, 044101 (2013)

Resonance mixing of alternating current magnetic fields in a multiferroic composite

*J. Appl. Phys.* **113**, 033902 (2013)

Improved dielectric and magnetic properties of Ti modified  $\text{BiCaFeO}_3$  multiferroic ceramics

*J. Appl. Phys.* **113**, 023908 (2013)

New multiferroics based on  $\text{Eu}_x\text{Sr}_{1-x}\text{TiO}_3$  nanotubes and nanowires

*J. Appl. Phys.* **113**, 024107 (2013)

Strong room temperature exchange bias in self-assembled  $\text{BiFeO}_3\text{--Fe}_3\text{O}_4$  nanocomposite heteroepitaxial films

*Appl. Phys. Lett.* **102**, 012905 (2013)

### Additional information on *Appl. Phys. Lett.*

Journal Homepage: <http://apl.aip.org/>

Journal Information: [http://apl.aip.org/about/about\\_the\\_journal](http://apl.aip.org/about/about_the_journal)

Top downloads: [http://apl.aip.org/features/most\\_downloaded](http://apl.aip.org/features/most_downloaded)

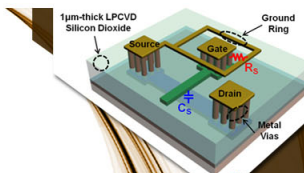
Information for Authors: <http://apl.aip.org/authors>

## ADVERTISEMENT



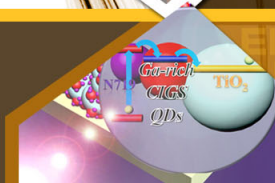
**EXPLORE WHAT'S  
NEW IN APL**

**SUBMIT YOUR PAPER NOW!**



### **SURFACES AND INTERFACES**

Focusing on physical, chemical, biological, structural, optical, magnetic and electrical properties of surfaces and interfaces, and more...



### **ENERGY CONVERSION AND STORAGE**

Focusing on all aspects of static and dynamic energy conversion, energy storage, photovoltaics, solar fuels, batteries, capacitors, thermoelectrics, and more...

# Magnetism and magnetoelectricity of a U-type hexaferrite $\text{Sr}_4\text{Co}_2\text{Fe}_{36}\text{O}_{60}$

K. Okumura,<sup>1</sup> T. Ishikura,<sup>1</sup> M. Soda,<sup>1,a)</sup> T. Asaka,<sup>2</sup> H. Nakamura,<sup>1</sup> Y. Wakabayashi,<sup>1</sup> and T. Kimura<sup>1,b)</sup>

<sup>1</sup>Division of Materials Physics, Graduate School of Engineering Science, Osaka University, Toyonaka, Osaka 560-8531, Japan

<sup>2</sup>Department of Materials Science and Engineering, Nagoya Institute of Technology, Nagoya 466-8555, Japan

(Received 25 March 2011; accepted 5 April 2011; published online 23 May 2011)

We report on structural, magnetic, and magnetoelectric (ME) properties of a U-type hexaferrite  $\text{Sr}_4\text{Co}_2\text{Fe}_{36}\text{O}_{60}$  prepared by solid state reaction. Samples sintered at 1150–1180 °C in oxygen contain the fewest impurity phases and show highly insulating behavior. Powder neutron diffraction results reveal that a commensurate magnetic order with a (0,0,3/2) propagation vector develops below  $T_{\text{N}2} \sim 350$  K. Corresponding to the appearance of the magnetic order, the sample shows a small ME effect. These results suggest that  $\text{Sr}_4\text{Co}_2\text{Fe}_{36}\text{O}_{60}$  is a room-temperature ME material in which the origin of the ME effect is similar to those of other ME hexaferrites. © 2011 American Institute of Physics. [doi:10.1063/1.3593371]

Ferrites, magnetic oxides containing iron as major metallic component, have contributed greatly to technological applications because of their room-temperature ferromagnetic and insulating properties.<sup>1,2</sup> Among such ferrites with various structures (e.g., spinels and garnets), ferrites with hexagonal structures, called *hexaferrites*, have long been used for permanent magnets and are of interest for microwave applications. The hexaferrites are classified into six main types depending on their chemical formulas and crystal structures: M-type  $(\text{Ba}, \text{Sr})\text{Fe}_{12}\text{O}_{19}$ , Y-type  $[(\text{Ba}, \text{Sr})_2\text{Me}_2\text{Fe}_{12}\text{O}_{22}]$ , W-type  $[(\text{Ba}, \text{Sr})\text{Me}_2\text{Fe}_{16}\text{O}_{27}]$ , Z-type  $[(\text{Ba}, \text{Sr})_3\text{Me}_2\text{Fe}_{24}\text{O}_{41}]$ , X-type  $[(\text{Ba}, \text{Sr})_2\text{Me}_2 \times \text{Fe}_{28}\text{O}_{46}]$ , and U-type  $[(\text{Ba}, \text{Sr})_4\text{Me}_2\text{Fe}_{36}\text{O}_{60}]$  ( $\text{Me}$  = divalent metal ion).<sup>1,3,4</sup> Their crystal structures can be described as stacked sequences of the basic blocks: S (spinel block), R  $[(\text{Ba}, \text{Sr})\text{Fe}_6\text{O}_{11}]^{2-}$ , and T  $(\text{Ba}, \text{Sr})_2\text{Fe}_8\text{O}_{14}$ . For example, the Y-type structure can be considered as an alternating stacking of the S and the T blocks along the hexagonal  $c$  axis.

Recent discoveries of low-field magnetoelectric (ME) effects in some Y-type and M-type hexaferrites<sup>5–9</sup> have ignited renewed interest in the study of hexaferrite materials. Furthermore, a Z-type hexaferrite  $\text{Sr}_3\text{Co}_2\text{Fe}_{24}\text{O}_{41}$  has been found to exhibit a low-field ME effect at room temperature.<sup>10,11</sup> In this letter, we report on structural, magnetic, and ME properties of a U-type hexaferrite  $\text{Sr}_4\text{Co}_2\text{Fe}_{36}\text{O}_{60}$ . The U-type structure<sup>12–14</sup> with the space group  $R\bar{3}m$  can be described as the sequence  $(\text{RSR}^*\text{S}^*\text{TS}^*)_3$ , where the  $(*)$  symbol means that the corresponding block turns 180° about the hexagonal  $c$  axis. We found that polycrystalline samples prepared by the solid state reaction show a small but finite ME effect up to  $\sim 350$  K, meaning that the U-type hexaferrite is a new room-temperature ME material.

Polycrystalline samples of  $\text{Sr}_4\text{Co}_2\text{Fe}_{36}\text{O}_{60}$  were prepared by the following procedures. First, powders of  $\text{SrCO}_3$ ,  $\text{Co}_3\text{O}_4$ , and  $\text{Fe}_2\text{O}_3$  were weighed to the prescribed ratios, mixed and well ground. The mixture was calcined at

1000 °C for 10 h and then pulverized. The resulting powders were put into rubber-walled tubes and isostatically cold-pressed under 40 MPa into rods (about 6 mm in diameter and 5 cm in length). The obtained rods were sintered for 16 h at 1150 or 1180 °C in air or in a flow of oxygen. Subsequently, they were slowly cooled down to room temperature for about 22 h in the oxygen atmosphere. Powder x-ray diffraction (XRD) measurements on the obtained specimens were carried out using  $\text{Cu } K\alpha$  radiation. For measurements of magnetization  $M$  and ME effect, the sintered rods were cut into thin plates with typical dimensions of  $\sim 40 \text{ mm}^2 \times \sim 0.5 \text{ mm}$ . The  $M$  was measured with a commercial magnetometer. For measurements of the electric polarization  $P$ , silver electrodes were evaporated onto the widest faces of the specimens. The magnetic-field  $B$  dependence of  $P$  was obtained by measurements of ME current.

Figure 1 shows powder XRD patterns of the obtained samples. Powder XRD data of Z-type  $\text{Sr}_3\text{Co}_2\text{Fe}_{24}\text{O}_{41}$  (Ref.

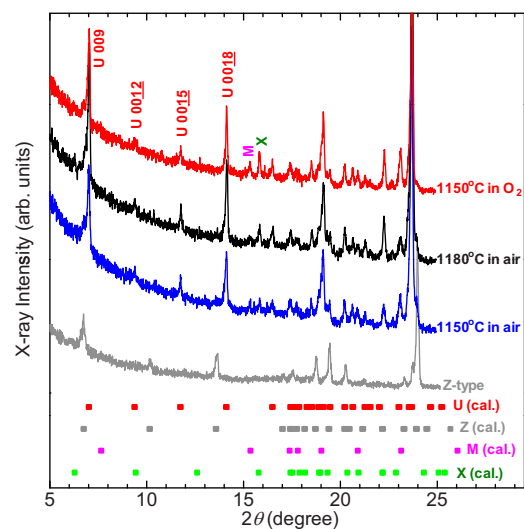


FIG. 1. (Color online) Powder XRD patterns of samples sintered at 1150 and 1180 °C in air and in a flow of oxygen. XRD data of Z-type  $\text{Sr}_3\text{Co}_2\text{Fe}_{24}\text{O}_{41}$  are also shown for comparison. The rectangles at the bottom represent the calculated peak positions for the U-, Z-, M-, and X-type structures.

<sup>a)</sup>Present address: Institute for Solid State Physics, University of Tokyo, Kashiwa 277-8581, Japan.

<sup>b)</sup>Electronic mail: kimura@mp.es.osaka-u.ac.jp.

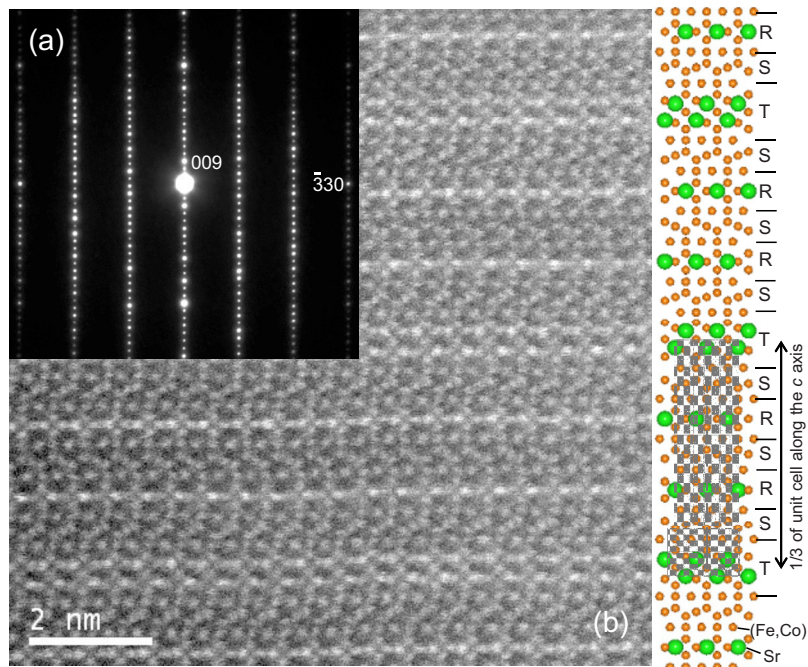


FIG. 2. (Color online) (a)  $[110]$  zone-axis ED pattern of  $\text{Sr}_4\text{Co}_2\text{Fe}_{36}\text{O}_{60}$  at room temperature. (b) Atomically resolved HAADF image taken along the  $[110]$  direction. A schematic drawing of the corresponding crystal structure is shown on the right side.

10) as well as the calculated peak positions for the U-, Z-, M-, and X-type structures are also shown for comparison. In the samples sintered in both air and oxygen atmosphere, most of the peaks can be indexed on the U-type structure with the space group  $R\bar{3}m$  and lattice parameters  $a = 5.86$  Å and  $c = 112.3$  Å, which demonstrates that the majority phase of these samples is U-type  $\text{Sr}_4\text{Co}_2\text{Fe}_{36}\text{O}_{60}$ . There are some impurity-peaks which can be indexed by the M- or X-type structure. However, no Z-type phase was observed as an impurity phase in our experimental resolution.

Pulverized specimens obtained from the sample sintered at 1150 °C in oxygen were examined using a transmission electron microscope (TEM) (JEM 2100F, JEOL Ltd., Tokyo, Japan). We obtained electron diffraction (ED) patterns and high-angle annular dark-field scanning TEM (HAADF-STEM) images for a total 11 grains. The results showed that all of the grains have the well-defined U-type structure. Figure 2 displays a typical ED pattern and HAADF-STEM image taken along the  $[110]$  zone-axis direction. In the HAADF-STEM image, heavy atoms such as Sr emerge as bright spots. Thus, the image is in good agreement with the U-type structure illustrated in the right panel of Fig. 2. Furthermore, no stacking fault or intergrowth was observed in the U-type grains, which was also evidenced by the absence of streaks in the ED pattern.

To investigate magnetic properties of the U-type  $\text{Sr}_4\text{Co}_2\text{Fe}_{36}\text{O}_{60}$ , powder neutron diffraction (ND) measurements were carried out using an ISSP triple axis spectrometer PONTA (incident neutron energy  $E_i = 14.7$  meV). The sample sintered at 1180 °C in air was set in an Al can filled with thermal exchange He gas, which was attached to the head of a Displex type refrigerator equipped with a high-power heater. Figure 3 shows ND patterns measured at 20, 450, and 650 K. Here, we focus on three prominent peaks at  $2\theta \approx 21.5^\circ$ ,  $23.5^\circ$ , and  $26.7^\circ$ . Considering the U-type structure, the  $21.5^\circ$  and  $23.5^\circ$  peaks are located at the 0018 and 0019.5 positions, respectively. The  $26.7^\circ$  peak corresponds to the 100, 101, 102, and 103 reflections. Since these four reflections are too close to each other, we term them “10L

peak.” Temperature ( $T$ ) profiles of the peak intensities of these reflections are displayed in the inset of Fig. 3. For comparison, the  $M$ - $T$  curve measured at 0.01 T is also shown. The  $M$ - $T$  curve exhibits a steep rise of  $M$  toward lower temperatures at  $T_{N1} \sim 690$  K where the 10L peak rapidly increases. As  $T$  decreases down to  $\sim 370$  K, the intensity of the 10L peak increases while those of 0018 and 0019.5 remain negligibly small. These results suggest that a ferrimagnetic ordering occurs at  $T_{N1}$  and that only the  $c$ -axis component of the ordered magnetic moments develops down to  $\sim 370$  K. As  $T$  is further decreased,  $M$  exhibits another steep rise at  $\sim 370$  K and then shows a maximum at  $T_{N2} \sim 350$  K. Around  $T_{N2}$ , the peak intensity of 10L also shows a maximum and those of 0018 and 0019.5 start to develop. The appearance of the 0019.5 reflection means that a magnetic ordering with the propagation vector  $\mathbf{q}_m = (0, 0, 3/2)$  develops below  $T_{N2}$ . Considering these ND results as well as those of some hexaferrites such as Y-type  $\text{Ba}_2\text{Mg}_2\text{Fe}_{12}\text{O}_{22}$  (Ref. 15) and Z-type  $\text{Sr}_3\text{Co}_2\text{Fe}_{24}\text{O}_{41}$  (Ref. 11), we speculate

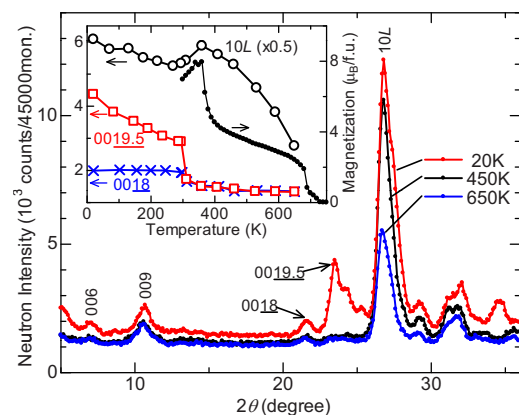


FIG. 3. (Color online) Powder ND patterns of  $\text{Sr}_4\text{Co}_2\text{Fe}_{36}\text{O}_{60}$  measured at 20, 450, and 650 K. (Inset) Temperature dependence of the peak intensities of the 10L peak, the 0018 and 0019.5 reflections. Temperature dependence of the magnetization measured at 0.01 T is also shown.



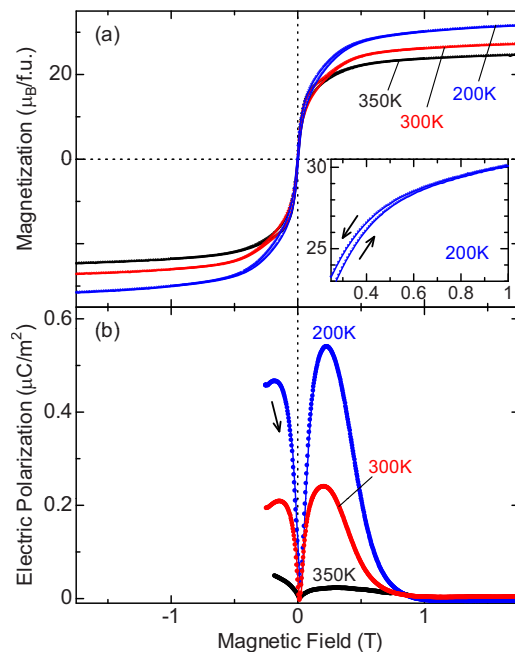


FIG. 4. (Color online) Magnetic-field dependence of (a) magnetization and (b) electric polarization at selected temperatures for a postannealed sample of  $\text{Sr}_4\text{Co}_2\text{Fe}_{36}\text{O}_{60}$ . Inset of (a): an expanded view of the data at 200 K.

that the magnetic moments are rotated toward the  $c$  plane and form a conical order below  $T_{\text{N}2}$ .

To obtain highly insulating samples for ME measurements, a sample sintered at 1150 °C in oxygen was postannealed at 1000 °C and then cooled down to room temperature in oxygen for about 24 h. The obtained sample showed no change in its XRD pattern and possesses high resistivity ( $\sim 4 \text{ G}\Omega \text{ cm}$  at room temperature). Figure 4 shows the  $B$  dependence of (a)  $M$  and (b)  $P$  at selected temperatures for the sample. For measurements of  $P$ , the sample was first poled by the following procedure. To begin,  $B$  of  $-3 \text{ T}$  was applied. Then, an electric field ( $E_{\text{pole}} \sim +0.4 \text{ MV/m}$ ) was applied perpendicular to  $B$ . Subsequently,  $B$  was set to  $-0.25 \text{ T}$ . After these poling procedures,  $E_{\text{pole}}$  was removed. Then, the ME current  $I_{\text{ME}}$  was measured with an electrometer while sweeping  $B$  at a rate of  $+1 \text{ T/min}$ . The  $P$  was obtained from the integration of  $I_{\text{ME}}$  by time. As seen in Fig. 4(a), the  $M$ - $B$  curves show a small but substantial hysteresis. The hysteresis vanishes at  $|B| > 0.6$  or  $0.7 \text{ T}$  [see the inset of Fig. 4(a)], and then  $M$  is nearly saturated above  $|B| \sim 0.8 \text{ T}$ . The  $B$  dependence of  $P$  reveals the ME coupling. As displayed in Fig. 4(b), there is almost no spontaneous  $P$  at  $B = 0$ . By applying  $B$ ,  $P$  appears and shows a rapid increase up to  $0.2$ – $0.3 \text{ T}$ . With the further increase in  $B$ ,  $P$  reaches a

maximum at  $0.2$ – $0.3 \text{ T}$  and then starts to decrease. Finally,  $P$  vanishes at  $0.7$ – $0.8 \text{ T}$  where  $M$  is almost saturated. However,  $P$  at  $350 \text{ K}$  is drastically suppressed in all the  $B$  range. These results demonstrate that U-type  $\text{Sr}_4\text{Co}_2\text{Fe}_{36}\text{O}_{60}$  exhibits the ME effect at a wide range of temperatures below  $T_{\text{N}2} \sim 350 \text{ K}$ , though the  $B$ -induced  $P$  at room temperature ( $\sim 0.2 \mu\text{C/m}^2$ ) is two orders of magnitude less than that in Z-type  $\text{Sr}_3\text{Co}_2\text{Fe}_{24}\text{O}_{41}$  (Ref. 10).

In summary, we investigated structural, magnetic, and ME properties of polycrystalline samples of a U-type hexaferrite  $\text{Sr}_4\text{Co}_2\text{Fe}_{36}\text{O}_{60}$ . Corresponding to the appearance of the magnetic order with the propagation vector  $(0,0,3/2)$ , a small ME effect was observed below  $T_{\text{N}2} \sim 350 \text{ K}$ . These results suggest that  $\text{Sr}_4\text{Co}_2\text{Fe}_{36}\text{O}_{60}$  is a room-temperature ME material with the same ME mechanism as other ME hexaferrites.

We thank T. Takeuchi, Y. Hiraoka, T. Honda, T. Usui, and Y. Yamaguchi for their help in experiments. Work at the JRR-3 was supported by ISSP of University of Tokyo. Work by TA was supported by a grant from Institute of Ceramics Research and Education, Nagoya Institute of Technology. This work was supported by KAKENHI (Grant Nos. 20674005, 20001004, 19052001, and 19052002) and the Global COE Program (G10).

<sup>1</sup>J. Smit and H. P. J. Wijn, *Ferrites* (Phillips Technical Library, Eindhoven, The Netherlands, 1959).

<sup>2</sup>S. Sugimoto, *J. Am. Ceram. Soc.* **82**, 269 (1999).

<sup>3</sup>P. B. Braun, *Philips Res. Rep.* **12**, 491 (1957).

<sup>4</sup>J. A. Kohn, D. W. Eckart, and C. F. Cook, Jr., *Science* **172**, 519 (1971).

<sup>5</sup>T. Kimura, G. Lawes, and A. P. Ramirez, *Phys. Rev. Lett.* **94**, 137201 (2005).

<sup>6</sup>S. Ishiwata, Y. Taguchi, H. Murakawa, Y. Onose, and Y. Tokura, *Science* **319**, 1643 (2008).

<sup>7</sup>K. Taniguchi, N. Abe, S. Ohtani, H. Umetsu, and T. Arima, *Appl. Phys. Express* **1**, 031301 (2008).

<sup>8</sup>S. H. Chun, Y. S. Chai, Y. S. Oh, D. Jaiswal-Nagar, S. Y. Haan, I. Kim, B. Lee, D. H. Nam, K.-T. Ko, J. H. Park, J.-H. Chung, and K. H. Kim, *Phys. Rev. Lett.* **104**, 037204 (2010).

<sup>9</sup>Y. Tokunaga, Y. Kaneko, D. Okuyama, S. Ishiwata, T. Arima, S. Wakimoto, K. Kakurai, Y. Taguchi, and Y. Tokura, *Phys. Rev. Lett.* **105**, 257201 (2010).

<sup>10</sup>Y. Kitagawa, Y. Hiraoka, T. Honda, T. Ishikura, H. Nakamura, and T. Kimura, *Nature Mater.* **9**, 797 (2010).

<sup>11</sup>M. Soda, T. Ishikura, H. Nakamura, Y. Wakabayashi, and T. Kimura, *Phys. Rev. Lett.* **106**, 087201 (2011).

<sup>12</sup>A. J. Kerecman, A. Tauber, T. R. Aucoin, and R. O. Savage, *J. Appl. Phys.* **39**, 726 (1968).

<sup>13</sup>R. C. Pullar and A. K. Bhattacharya, *J. Mater. Sci.* **36**, 4805 (2001).

<sup>14</sup>D. Lisjak, D. Makovec, and M. Drofenik, *J. Mater. Res.* **19**, 2462 (2004).

<sup>15</sup>S. Ishiwata, D. Okuyama, K. Kakurai, M. Nishi, Y. Taguchi, and Y. Tokura, *Phys. Rev. B* **81**, 174418 (2010).